Kinetics of Tautomerism in 2-Substituted 5,10,15,20-Tetraphenylporphyrins: Directionality of Proton Transfer between the Inner Nitrogens[1]

Maxwell J. Crossley,* Leslie D. Field,* Margaret M. Harding, and Sever Sternhell

Contribution from the Department of Organic Chemistry, The University of Sydney, N.S.W. 2006, Australia. *Received August 11, 1986*

Abstract: The kinetics of tautomerism in a range of 2-substituted 5,10,15,20-tetraphenylporphyrins **9–18** was studied by NMR spectroscopy using saturation transfer experiments and line shape analysis of the N–H resonances of the 400-MHz ^{1}H NMR spectra. Intermolecular proton transfer between porphyrin and porphyrin or porphyrin and solvent molecules at 310 K was excluded by saturation transfer experiments, and the dynamic behavior of the N–H resonances was interpreted solely in terms of intramolecular transfer of the two hydrogens between the four inner nitrogens. Two distinct energy barriers for proton transfer were measured. At low temperatures (<200 K), equilibrium saturation transfer experiments and saturation transfer inversion–recovery experiments on **9–18** indicated that the only significant exchange on the NMR time scale involves a net transfer of one hydrogen between N-24 and N-21 and the second hydrogen between N-22 and N-23. Alternate processes (e.g., transfer of the hydrogens between N-21 and N-22 and between N-23 and N-24) were either minor or not detected. This directionality of proton transfer was confirmed by line shape analysis of the N–H resonances of **9–18** in the temperature range 200–250 K. Spectra were simulated with proton transfer restricted to exchange between N-24 and N-21 and between N-22 and N-23 for porphyrins where R = CH_3, NH_2, $CH{=}CH_2$, CH_2OH, $NHCOCH_3$, OCH_3, and SPh. The free energy of activation for this process at 255 K is $\Delta G_1^{\ddagger} = 46.6 \pm 1.2$ kJ·mol^{-1}. This energy barrier is apparently independent of the electronic nature of the substituent. Above 250 K, net proton transfer between N-24 and N-23 and between N-22 and N-21 is also observable on the NMR time scale and contributes to the spectral line shape. Measurement of this higher energy barrier ($\Delta G_2^{\ddagger}$) was restricted to those porphyrins in which the dominant tautomer contains the R group substituted on the aromatic delocalization pathway (i.e., **2b**) and was measured when R = NH_2 and CH_3 ($\Delta G_2^{\ddagger} = 56.7 \pm 0.9$ kJ·mol^{-1}). The cause of the directionality of the tautomerism is discussed in terms of steric and electronic effects. The deuterium isotope effect for the proton transfers N-21 → N-24 and N-22 → N-23 (30 ± 3) in 2-methoxy-5,10,15,20-tetraphenylporphyrin **9** is similar to values reported for the unsubstituted 5,10,15,20-tetraphenylporphyrin. Arrhenius plots of the kinetic data were linear over the range 200–300 K and show no evidence of proton tunneling. The magnitudes of the activation parameters are similar to results reported for other tetraarylporphyrins, which suggests that the mechanism of the proton transfer is similar.

The tautomeric exchange involving inner hydrogen migration is an important fundamental property of porphyrins which has been the subject of numerous studies.[2-15] The exchange is also an excellent model for cyclic proton-transfer reactions since the two "reactants" are held together by the porphyrin skeleton.[10] Each porphyrin tautomer (e.g., **1a** ⇄ **1b**) contains an 18π-electron delocalization pathway with two isolated double bonds on the periphery. The tautomeric exchange is rapid on the NMR time scale at room temperature but has been observed in solution by proton,[2,4a,c,5-8,10,15] carbon-13,[3,4] and nitrogen-15[6-9] variable-temperature NMR spectroscopies. The presence of tautomerism in the solid state has also been established.[10h]

The bulk of the experimental and theoretical work on tautomerism in porphyrins has involved symmetrical systems, and most of the previous studies have centered on 5,10,15,20-tetraphenylporphyrin **1**. However, while activation parameters for the exchange **1a** ⇄ **1b** have been determined by line shape analysis of proton,[2,4c,10a] carbon-13,[4a,c] and nitrogen-15 NMR spectra,[9,10a] the mechanism of the proton transfer has not been established unequivocally. Proton transfer occurs entirely by an intramolecular process,[5,8] and the energetics of the exchange have been interpreted in a number of different ways.

Three aspects have received particular attention: the extent of synchronism in the central proton-transfer movement, the degree of distortion of the porphyrin skeleton that accompanies the transfer, and the contribution of proton tunneling. Simultaneous proton transfer via a symmetrical transition state has been proposed on the basis of isotope effects and activation parameters.[2,4a,c,5,9] Stepwise migration of the protons has been discounted on the basis that it would involve a high-energy intermediate or transition state in which the inner hydrogens are bonded to adjacent nitrogens.[12] Several studies have addressed the problem of possible proton tunneling at low temperatures[10,11] and proposed that the migration takes place by tunneling between quantized

(1) Presented in part at the Eighth National Conference of the Division of Organic Chemistry of the Royal Australian Chemical Institute, Perth, May, 1984.

(2) (a) Storm, C. B.; Teklu, Y. *J. Am. Chem. Soc.* **1972**, *94*, 1745. (b) Storm, C. B.; Teklu, Y.; Sokoloski, R. *Ann. N. Y. Acad. Sci.* **1973**, *206*, 631.

(3) Matwiyoff, N. A.; Burnham, B. F. *Ann. N. Y. Acad. Sci.* **1973**, *206*, 365.

(4) (a) Abraham, R. J.; Hawkes, G. E.; Smith, K. M. *Tetrahedron Lett.* **1974**, 1483. (b) Abraham, R. J.; Hawkes, G. E.; Smith, K. M. *J. Chem. Soc., Perkin Trans. 2* **1974**, 627. (c) Abraham, R. J.; Hawkes, G. E.; Hudson, M. F.; Smith, K. M. *J. Chem. Soc., Perkin Trans. 2* **1975**, 204.

(5) Eaton, S. S.; Eaton, G. R. *J. Am. Chem. Soc.* **1977**, *99*, 1601.

(6) Irving, C. S.; Lapidot, A. *J. Chem. Soc., Chem. Commun.* **1977**, 184.

(7) (a) Kawano, K.; Ozaki, Y.; Kyogoku, Y.; Ogoshi, H.; Sugomoto, H.; Yoshida, Z.-I. *J. Chem. Soc., Chem. Commun.* **1977**, 226. (b) Kawano, K.; Ozaki, Y.; Kyogoku, Y.; Ogoshi, H.; Sugomoto, H.; Yoshida, Z.-I. *J. Chem. Soc., Perkin Trans. 2* **1978**, 1319.

(8) Yeh, H. J. C.; Sato, M.; Morishima, I. *J. Magn. Reson.* **1977**, *26*, 365.

(9) Gust, D.; Roberts, J. D. *J. Am. Chem. Soc.* **1977**, *99*, 3637.

(10) (a) Limbach, H.-H.; Hennig, J. *J. Chem. Soc., Faraday Trans. 2* **1979**, *75*, 752. (b) Limbach, H.-H.; Hennig, J. *J. Chem. Phys.* **1979**, *71*, 3120. (c) Hennig, J.; Limbach, H.-H. *J. Magn. Reson.* **1982**, *49*, 322. (d) Limbach, H.-H.; Hennig, J.; Gerritzen, D.; Rumpel, H. *Faraday Discuss. Chem. Soc.* **1982**, *74*, 229. (e) Limbach, H.-H.; Hennig, J.; Stulz, J. *J. Chem. Phys.* **1983**, *78*, 5432–5436. (f) Hennig, J.; Limbach, H.-H. *J. Am. Chem. Soc.* **1984**, *106*, 292. (g) Limbach, H.-H. *J. Chem. Phys.* **1984**, *80*, 5343. (h) Limbach, H.-H.; Hennig, J.; Kendrick, R.; Yannoni, C. S. *J. Am. Chem. Soc.* **1984**, *106*, 4059.

(11) (a) Stilbs, P.; Moseley, M. E. *J. Chem. Soc., Faraday Trans. 2* **1980**, *76*, 729. (b) Stilbs, P. *J. Magn. Reson.* **1984**, *58*, 152.

(12) (a) Sarai, A. *Chem. Phys. Lett.* **1981**, *83*, 50. (b) Sarai, A. *J. Chem. Phys.* **1982**, *76*, 5554. (c) Sarai, A. *J. Chem. Phys.* **1984**, *80*, 5341.

(13) Bersuker, G. I.; Polinger, V. Z. *Chem. Phys.* **1984**, *86*, 57.

(14) Butcher, R. J.; Jameson, G. B.; Storm, C. B. *J. Am. Chem. Soc.* **1985**, *107*, 2978.

(15) (a) Crossley, M. J.; Harding, M. M.; Sternhell, S. *J. Am. Chem. Soc.* **1986**, *108*, 3608. (b) Harding, M. M. Ph.D. Thesis, The University of Sydney, 1986.

(16) Schlabach, M.; Wehrle, B.; Limbach, H.-H.; Bunnenberg, E.; Knierzinger, A.; Shu, A. Y. L.; Tolf, B.-R.; Djerassi, C. *J. Am. Chem. Soc.* **1986**, *108*, 3856.

0002-7863/87/1509-2335$01.50/0

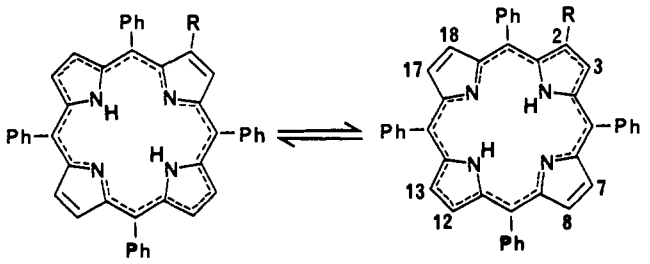

1a, R = H
2a, R = X

1b, R = H
2b, R = X

3, R = CN
4, R = NO_2
5, R = OCOPh
6, R = Cl
7, R = Br
8, R = CHO
9, R = OCH_3
10, R = SPh
11, R = $NHCOCH_3$
12, R = OH
13, R = CH_2OH
14, R = $CH{=}CH_2$
15, R = NH_2
16, R = *n*-Bu
17, R = CH_3
18, R = *i*-Pr

NH stretching states.[10] In addition, other models for the transfer have been proposed on the basis of calculations.[12]

While tautomerism in several asymmetric systems has been reported,[4a,6,15,17] kinetic data are limited. The study of such systems would be expected to provide much more information than is available from the study of symmetrical systems. Recently, we reported a study of the thermodynamics of proton transfer in 2-substituted 5,10,15,20-tetraphenylporphyrins **2**.[15,17] The asymmetry in **2** removes the degeneracy of the two tautomers of the porphyrin, **2a** and **2b**. Such nondegeneracy of porphyrin tautomers has only previously been observed in the solid state of triclinic 5,10,15,20-tetraphenylporphyrin and was the result of unequal crystal packing forces.[10h] Evidence for tautomerism in a triply ^{15}N labeled monoacetylporphyrin which also involved unequal tautomer populations has recently been reported.[16]

This paper describes a study of the kinetics of proton transfer in 2-substituted 5,10,15,20-tetraphenylporphyrins **2**. Variable-temperature NMR studies on 16 2-substituted porphyrins, **3–18**, showed that the position[15] of the tautomeric equilibrium is altered by the substituent and that the tautomerism can be readily monitored by variable-temperature NMR spectroscopy. Activation parameters for the tautomerism were determined by saturation transfer experiments and line shape analysis and compared to the values reported for the unsubstituted 5,10,15,20-tetraphenylporphyrin **1**.

Experimental Section

Dynamic NMR Spectroscopy. Proton NMR spectra were recorded on a Bruker WM 400 spectrometer in dry dideuteriodichloromethane, locked on solvent deuterium and referenced to the residual solvent peak. The temperature of the spectrometer probe was calibrated by the shift difference of methanol resonances in the ^1H NMR spectrum.[18] The data listed in Tables II and III were obtained by line shape analysis of the N–H resonances in porphyrins **9–18**. The line widths of the four N–H resonances were assumed equal. All chemical shifts were temperature dependent, and in the region where distinct resonances were not observed, the shifts were estimated by extrapolation of the shifts obtained at slow exchange. Activation parameters were obtained from weighted least-squares fits of the rate constants to the Arrhenius and Eyring equations.

Preparation of Porphyrins. The preparation of porphyrins **3–18** has been described previously.[15] 2-Methoxy-5,10,15,20-tetraphenylporphyrin was deuteriated (>98%) by three successive equilibrations in D_2O. The sample was dried over sodium sulfate prior to NMR analysis.

Results and Discussion

Our previous NMR studies[15] on porphyrins **3–18** showed that, in all cases, at low temperatures (<210 K), the tautomeric exchange **2a** ⇄ **2b** is slow on the NMR time scale and each tautomer gives rise to distinct sets of signals for the β-pyrrolic and N–H protons in the ^1H NMR spectrum. The N–H region (−2 to −4 ppm) of the NMR spectra of these porphyrins proved ideal for kinetic analysis since this region of the spectrum was well dispersed, was free of other resonances, and in general, exhibited four singlets at low temperatures.[15] Variable-temperature NMR spectra of all porphyrins **3–18** gave a series of spectra in which the four singlets present at low temperatures broadened and eventually coalesced into a singlet as the temperature was increased.

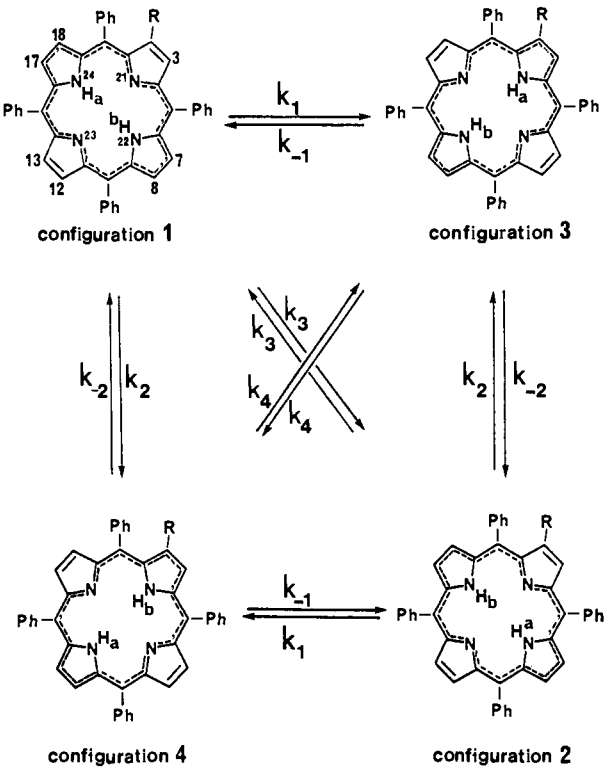

Figure 1. Intramolecular proton transfer between the four nuclear configurations in a 2-substituted 5,10,15,20-tetraphenylporphyrin.

Intermolecular Proton Transfer. The possibility that the dynamic behavior was a result of intermolecular proton transfer was excluded by NMR spectroscopy using saturation transfer experiments. At 310 K, the NMR spectrum of a mixture of 2-nitro-5,10,15,20-tetraphenylporphyrin **4** and 5,10,15,20-tetraphenylporphyrin **1** in dry CD_2Cl_2 contained two discrete N–H resonances (−2.64 and −2.80 ppm), which were assigned to **4** and **1**, respectively, by comparison with spectra of the individual compounds. Saturation of each N–H resonance in turn had no detectable effect on the signal intensity of the second resonance. Intermolecular proton exchange between solvent and porphyrin molecules was excluded in an analogous experiment; no saturation transfer was detected between the porphyrin N–H resonances and hydroxyl resonances (from residual water in the solvent) which were present in the NMR spectra of all porphyrins in CD_2Cl_2. These experiments indicate that the rate of intermolecular proton exchange is insignificant on the NMR time scale at 310 K, and hence intermolecular exchange was considered negligible below this temperature. Several studies on 5,10,15,20-tetraphenylporphyrin **1** have also demonstrated the absence of detectable intermolecular proton transfer in solution.[5,8]

Intramolecular Proton Transfer. With the possibility of intermolecular proton exchange eliminated, the dynamic behavior of the N–H resonances in the ^1H NMR spectra was attributed solely to intramolecular exchange processes.

In a 2-substituted 5,10,15,20-tetraphenylporphyrin, **2**, there are four sites which the two N–H protons can occupy, defined by the inner nitrogens N-21, N-22, N-23, and N-24. This gives rise to four distinct arrangements for the N–H protons, shown as configurations 1–4 in Figure 1. No evidence was found for stable

(17) The presence of tautomerism in asymmetric porphyrins creates a nomenclature problem which has not previously been addressed. Thus **2** exists as a mixture of a 2- and a 7-substituted tautomer. For clarity in this paper we have numbered both tautomers of **2** the same way; i.e., the substituent occupies the 2-position, and all other atoms retain the same number in both tautomers.

(18) Van Geet, A. L. *Anal. Chem.* **1970**, *42*, 679.

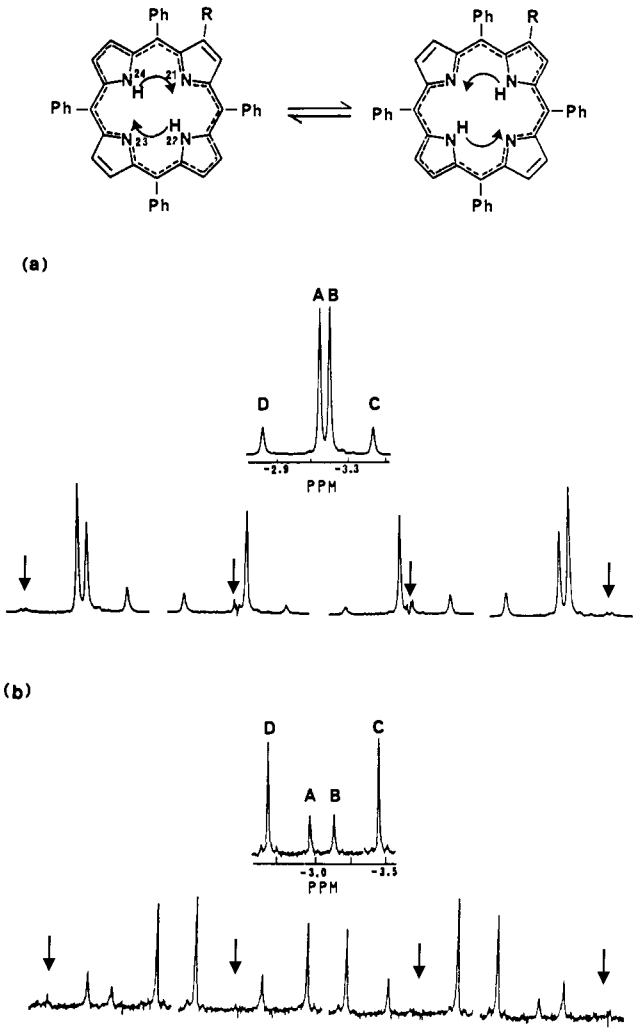

Figure 2. Saturation transfer in the N–H region of the 400-MHz ^{1}H NMR spectra of (a) 2-methoxy-5,10,15,20-tetraphenylporphyrin **9** (200 K) and (b) 2-amino-5,10,15,20-tetraphenylporphyrin **15** (189 K), in CD_2Cl_2. Arrows indicate the frequency of saturation. ν_A is the frequency of N-24–H, ν_B the frequency of N-22–H, ν_C the frequency of N-21–H, and ν_D the frequency of N-23–H.

tautomers in which the two hydrogens reside on adjacent nitrogens. Configurations 1 and 2 give identical NMR spectra since they differ only in the position of the two interior hydrogens which have exchanged sites. The protons at N-24 and N-22 appear as singlets at ν_A and ν_B, respectively, in the ^{1}H NMR spectrum. Similarly, configurations 3 and 4 contain a proton at each of the sites N-21 and N-23 and give rise to N–H resonances at ν_C and ν_D, respectively.

The N–H protons, at slow exchange, were assigned to their individual sites by decoupling experiments.[15] Irradiation at ν_A decoupled the AB quartet arising from $H_{17,18}$, while irradiation at ν_B decoupled the AB quartet arising from $H_{7,8}$.[15] Similarly, irradiation at ν_C decoupled the signal arising from H_3, while irradiation of ν_D enhanced the AB quartet arising from $H_{12,13}$.

Qualitative information as to the dominant exchange processes near slow exchange in porphyrins **9–18** was provided by saturation transfer experiments. Continuous saturation at any one of the four frequencies ν_A, ν_B, ν_C, or ν_D in porphyrins **9–18** resulted in new equilibrium intensities at the other three signals, reflecting the rate of magnetization transfer between the sites (Figure 2). Saturation at ν_A (i.e., the frequency of the proton at N-24) decreased the intensity of the signal at ν_C by up to 50% but had no detectable effect on the intensity of the signals at ν_B and ν_D; i.e., the proton at N-24 loses magnetization mainly by proton transfer to N-21. Similarly, saturation at ν_B resulted in a significant decrease in the signal intensity at ν_D but had no detectable effect on the intensities of the signals at ν_A and ν_C. Hence, the rate of proton transfer from N-22 to N-23 is large in comparison to the exchange from N-22 to N-21 or N-24. These results show that the dominant exchange below 200 K is as shown in Figure 2. The reverse experiments (saturation at ν_C and ν_D) confirmed this conclusion.

The "steady-state" saturation transfer experiment has been used to obtain rate constants in various exchanging systems.[19] However, due to the small differences in chemical shift of ν_A and ν_B (20 Hz), selective saturation at ν_A could not be achieved without partial saturation of the signal at ν_B, and accurate rate constants could not be obtained by this method.

In order to obtain quantitative rate data in this system, a saturation inversion–recovery experiment was used. In this experiment, one of the N–H resonances was saturated (or partially saturated) at $t = 0$ in order to establish nonequilibrium magnetizations at the four sites. The saturating field was turned off, and the NMR signals were inverted immediately with a nonselective composite 180° pulse.[20] The subsequent recovery of M_z^A, M_z^B, M_z^C, and M_z^D (i.e., the magnetization at ν_A, ν_B, ν_C, and ν_D, respectively) was monitored as a function of time after inversion.

The rate of recovery of each of the four resonances to equilibrium depends on the relaxation times (T_1) of the nuclei and the exchange processes. This method does not depend on selective saturation of one frequency, since the rate of recovery of magnetization in *any* nonequilibrium sample to equilibrium is governed by the Bloch equations modified to include chemical exchange.[21] The four configurations can be interconverted by the processes shown in Figure 1. From configuration 1 the protons may move in a clockwise direction to configuration 3 (k_1) or in an anticlockwise direction to give configuration 4 (k_2). Alternatively, configuration 1 may directly interchange to configuration 2 (k_3) and bypass the intermediates 3 and 4. Similar options exist for proton transfer from the other three configurations. The Bloch equations including all of these exchange processes can be formulated. However, the steady-state saturation transfer experiments indicated that k_2, k_{-2}, k_3, and k_4 are insignificant on the NMR time scale below 200 K, and this permits some simplification of eq 1–4.

$$\frac{dM_z^A}{dt} = \frac{-(M_z^A - M_0^A)}{T_1^A} - 2M_z^A k_1 + 2M_z^C k_{-1} \quad (1)$$

$$\frac{dM_z^B}{dt} = \frac{-(M_z^B - M_0^B)}{T_1^B} - 2M_z^B k_1 + 2M_z^D k_{-1} \quad (2)$$

$$\frac{dM_z^C}{dt} = \frac{-(M_z^C - M_0^C)}{T_1^C} - 2M_z^C k_{-1} + 2M_z^A k_1 \quad (3)$$

$$\frac{dM_z^D}{dt} = \frac{-(M_z^D - M_0^D)}{T_1^D} - 2M_z^D k_{-1} + 2M_z^B k_1 \quad (4)$$

When the system is at equilibrium, $dM_z^{A,B,C,D}/dt = 0$, $M_z^{A,B,C,D} = M_0^{A,B,C,D}$, $M_0^A = M_0^B$, and $M_0^C = M_0^D$. Substitution in eq 1–4, assuming T_1 at the four sites is equal, gives eq 5.

$$M_0^A k_1 = M_0^C k_{-1} \quad (5)$$

For a particular porphyrin sample at a given temperature, one of the N–H resonances was saturated. The saturating field was turned off, and a series of spectra were acquired by using a 180°–τ–90° pulse sequence to monitor the recovery of all four N–H resonances to equilibrium (e.g., Figure 3). The variable time delay, τ, was varied in 2-ms increments from 0 to 20 ms and then increased more rapidly to 5 s, where the system was at equilibrium. The data obtained from each of the four experiments performed on each compound (i.e., saturation of each N–H resonance followed by the inversion–recovery sequence) were fitted simultaneously to the integrated Bloch equations (eq 1–4) by using a generalized nonlinear least-squares computer program. The

(19) Hoffmann, R. A.; Fòrsen, S. *Progr. Nucl. Magn. Reson. Spectrosc.* **1966**, *1*, 15. (b) Fòrsen, S.; Hoffman, R. A. *J. Chem. Phys.* **1963**, *39*, 2892. (c) Fôrsen, S.; Hoffman, R. A. *J. Chem. Phys.* **1964**, *40*, 1189.
(20) Freeman, R.; Keeler, J. *J. Magn. Reson.* **1981**, *43*, 484.
(21) McConnell, H. M. *J. Chem. Phys.* **1958**, *28*, 430.

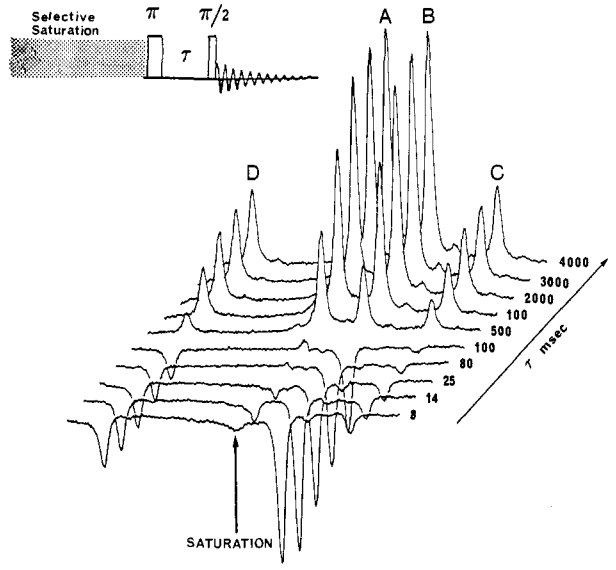

Figure 3. 400-MHz ^{1}H NMR spectra showing selective saturation at ν_A inversion–recovery in 2-acetamido-5,10,15,20-tetraphenylporphyrin **11**, in CD_2Cl_2 at 193 K.

Table I. Kinetic Data from Computer-Generated Curves of Best Fit to Equations 1–5 for Saturation Transfer Experiments

compd no.	R	T, K	P2a/P2b[a]	T_1, s	rate, s^{-1}[b]
11	$NHCOCH_3$	193	3.05 ± 0.11	0.65 ± 0.02	k_1 = 0.94 ± 0.11 k_{-1} = 2.87
9	OCH_3	192	4.67 ± 0.14	0.66 ± 0.005	k_1 = 0.66 ± 0.13 k_{-1} = 3.10
15	NH_2	187	0.33 ± 0.19	0.73 ± 0.005	k_1 = 1.84 ± 0.21 k_{-1} = 0.61

[a] Ratio of the tautomeric populations of **2**. [b] $k_{-1} = k_1(P2a/P2b)$.

equilibrium magnetizations, the relaxation time, and the rate constants were varied to provide curves of best fit to the data (e.g., Figure 4). This analysis was carried out on porphyrins **9**, **11**, and **15**, which afforded the rate constants k_1 and k_{-1} (Table I). These porphyrins were particularly suited for this analysis as the NMR spectra contained four peaks of sufficient population to provide accurate information in each of the recovery curves.

Application of the saturation transfer experiment is limited to systems in which the rates of exchange are of the same order of magnitude as the reciprocal of T_1.[20] Under the experimental conditions, T_1 for the N–H protons was ca. 0.7 s, and consequently only exchange rates less than ca. 3 s^{-1} could be measured by this technique. The experiments were carried out at a temperature where saturation of one of the N–H resonances arising from the minor tautomer reduced the signal intensity of one of the N–H resonances arising from the major tautomer by approximately 30%. At higher temperatures, where saturation transfer was more efficient, the data obtained were insensitive to the rate constants.

Line Shape Analysis. At temperatures higher than those where saturation transfer was applicable, proton exchange was followed by total line shape analysis. From the saturation transfer data it was apparent that only the processes defined by the rate constants k_1 and k_{-1} were important on the NMR time scale below 200 K. While it was possible that other rate constants contributed significantly to the spectral shape at higher temperatures, a total line shape analysis was initially performed assuming that k_1 and k_{-1} were the only rate constants responsible for the observed line broadening of the N–H resonances.

Line shape analysis of the N–H region of the NMR spectra of porphyrins **9**, **10**, **11**, **13**, **14**, **15**, and **17** was carried out by using the iterative computer program DNMR5.[22] The spectra were

(22) Stephenson, D. S.; Binsch, G. *J. Magn. Reson.* **1978**, *32*, 145.

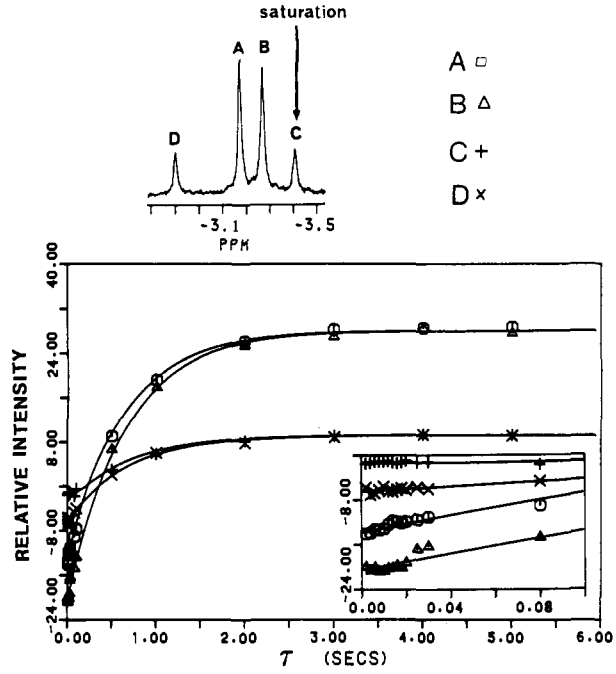

Figure 4. Computer-generated curves of best fit of NMR data for selective saturation at ν_C inversion–recovery using the pulse sequence shown in Figure 3 for 2-acetamido-5,10,15,20-tetraphenylporphyrin **11**, in CD_2Cl_2 at 193 K.

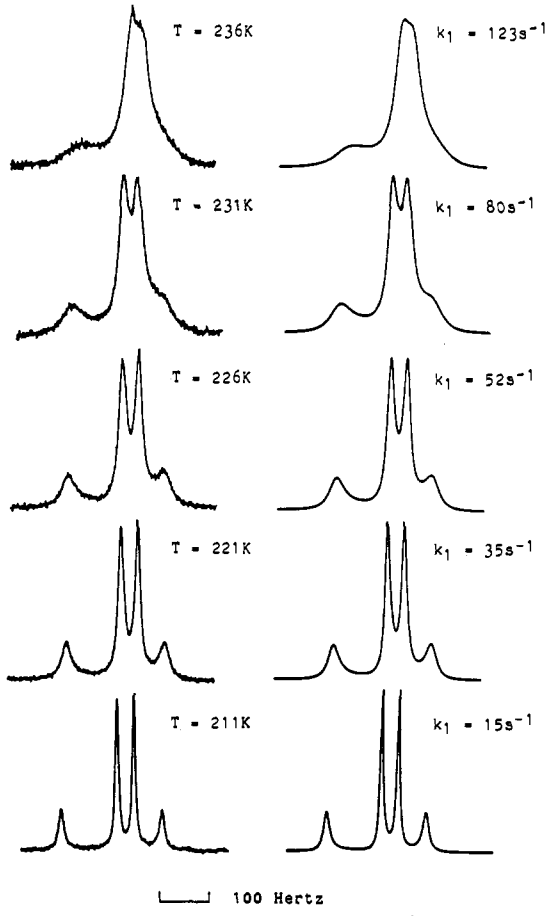

Figure 5. Experimental and calculated 400-MHz ^{1}H NMR spectra of 2-acetamido-5,10,15,20-tetraphenylporphyrin **11**, in CD_2Cl_2.

analyzed according to the processes defined in Figure 1, and excellent agreement between the experimental and calculated spectra over the range 200–250 K was obtained by simulating the spectra with only the two rate constants, k_1 and k_{-1}; i.e., proton transfer was restricted to exchanges N-24 ⇄ N-21 and N-22 ⇄

Table II. Activation Parameters for Proton Transfers N-24 → N-21 and N-22 → N-23

compd no.	R	temp range, K	*P2a*/*P2b*[a] (200 K)	$\Delta S^{\ddagger}$, J·K^{-1}·mol^{-1}	$\Delta H^{\ddagger}$, kJ·mol^{-1}	$\Delta G_1^{\ddagger}{}_{225}$, kJ·mol^{-1}
17	CH_3	191–251	0.30	−82.1 ± 3.3	26.4 ± 0.7	44.9 ± 0.6
15	NH_2	201–251	0.48	−74.8 ± 3.2	28.7 ± 0.7	45.6 ± 0.6
14	$CH{=}CH_2$	196–241	0.58	−68.0 ± 7.9	30.4 ± 1.7	45.7 ± 0.6
13	CH_2OH	211–246	0.61	−45.0 ± 6.5	35.7 ± 1.5	45.8 ± 0.6
11	$NHCOCH_3$	201–241	2.16	−74.2 ± 6.1	30.5 ± 1.4	47.2 ± 0.7
9	OCH_3	211–236	3.17	−81.0 ± 4.1	29.6 ± 0.9	47.8 ± 0.7
10	SPh	201–241	3.32	−82.8 ± 8.5	28.5 ± 1.9	47.1 ± 0.7

[a] Ratio of the tautomeric populations of **2**.

Table III. Activation Parameters for Proton Transfers N-24 → N-23 and N-22 → N-21

compd no.	R	temp range, K	*P2a*/*P2b*[a] (270 K)	$\Delta S^{\ddagger}$, J·K^{-1}·mol^{-1}	$\Delta H^{\ddagger}$, kJ·mol^{-1}	$\Delta G_2^{\ddagger}{}_{280}$, kJ·mol^{-1}
17	CH_3	261–291	0.33	−89.1 ± 4.5	31.8 ± 1.3	56.8 ± 0.8
15	NH_2	267–298	0.56	−42.8 ± 3.6	44.6 ± 1.0	56.6 ± 0.7

[a] Ratio of the tautomeric populations of **2**.

N-23 (Figure 5). These results are entirely consistent with the conclusions reached from the saturation transfer experiments; i.e., at low temperatures the line shape of the N–H protons is dominated by two rate constants, k_1 and k_{-1}.

However, at temperatures > 250 K, the spectra could not be simulated with only the two rate constants k_1 and k^{-1}. This was apparent from the experimental spectra of porphyrins **3–18**, since at fast exchange (>300 K) the N–H protons appeared as a broad singlet. The simulations indicated that at fast exchange, when k_1 and k_{-1} are the only significant rate constants present, the spectra should consist of two singlets centered at the population-weighted averages of ν_A and ν_C and of ν_B and ν_D. The spectra of the N–H resonances of most of the porphyrins studied had collapsed to a singlet by 260 K, but in porphyrins **15**, **17**, and **18**, two singlets centered at the population-weighted averages of ν_A and ν_C and of ν_B and ν_D appeared in the range 260–270 K. However, these peaks coalesced at higher temperatures, and in all porphyrins studied in this work, the N–H region of the spectrum appeared as a broad singlet at 310 K.

Since the contribution of intermolecular proton transfer to the observed line shape was negligible at these temperatures, the additional exchange process apparent in the spectra of porphyrins **15**, **17**, and **18** was attributed to the contribution from the intramolecular proton transfers N-24 ⇄ N-23 and N-22 ⇄ N-21, i.e., k_2 and k_{-2}. In principle, the additional exchange observed could also be attributed to the rate constants k_3 and k_4; however, this was considered highly unlikely since this exchange requires that the protons move out of the plane of the porphyrin and across a larger distance.[23]

Full analysis of proton transfer over the entire range 200–298 K was carried out on porphyrins **15** and **17**. Spectra between 200 and 250 K were calculated with the two rate constants k_1 and k_{-1}. Values of k_1 and k_{-1} at higher temperatures were estimated by extrapolation from the lower temperature domain. Values of k_2 required to give good simulations of the experimental spectrum were computed by DNMR5[22] (Figure 6).

Values of k_2 and k_{-2} could not be obtained by line shape analysis in porphyrins where **2a** is the major tautomer, i.e., **9**, **10**, and **11**. This was a consequence of the fact that above 250 K the population-weighted averages of ν_A and ν_C and of ν_B and ν_D were coincident. Hence, the spectral line shape was insensitive to the rate constants at higher temperatures. In contrast, in porphyrins **13**, **15**, and **17**, where **2b** is the major tautomer, two peaks corresponding to the population-weighted averages of ν_A and ν_C and of ν_B and ν_D were resolved in the temperature range 240–260 K.

Activation Parameters. Two activation energies were measured in this work, $\Delta G_1^{\ddagger}$ and $\Delta G_2^{\ddagger}$ (Figure 7). The free energy of activation, $\Delta G_1^{\ddagger}$, for proton transfer from N-24 to N-21 and from N-22 to N-23 (k_1 rate process) was measured in porphyrins **9**, **10**, **11**, **13**, **14**, **15**, and **17**. The free energy of activation, $\Delta G_2^{\ddagger}$, for proton transfer from N-24 to N-23 and from N-22 to N-21 (k_2 rate process) was measured in porphyrins **15** and **17**.[24]

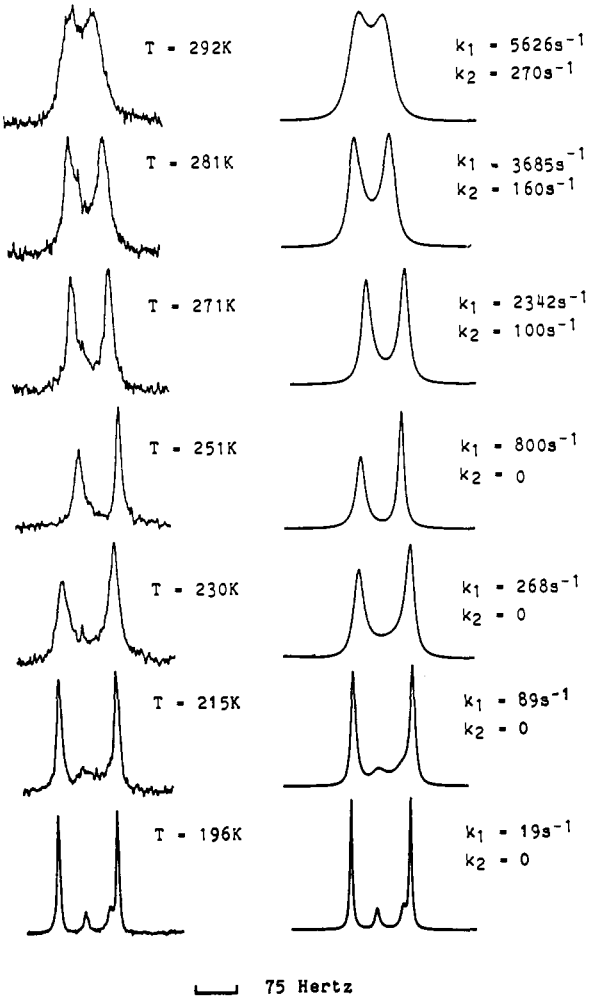

Figure 6. Experimental and calculated 400-MHz ^{1}H NMR spectra of 2-methyl-5,10,15,20-tetraphenylporphyrin **17**, in CD_2Cl_2.

The kinetic and thermodynamic parameters from the measurement of k_1 and k_2 at 225 and 280 K, respectively, are summarized in Tables II and III. In order to compare the two

(23) The exchange defined by k_3 (and k_4) involves proton movements of ca. 2.4 Å (obtained by using a transannular N···N separation of 4.19 Å and an N–H distance of 0.9 Å)[14] compared with 1.84 Å for sideways movement to the adjacent nitrogen.[10b]

(24) The activation parameters for proton transfer in the opposite direction (i.e., k_{-1} and k_{-2} rate processes) are also available from the data. However, these barriers are related to $\Delta G_1^{\ddagger}$ and $\Delta G_2^{\ddagger}$ and differ only by a factor which reflects the ratio of the tautomeric populations.

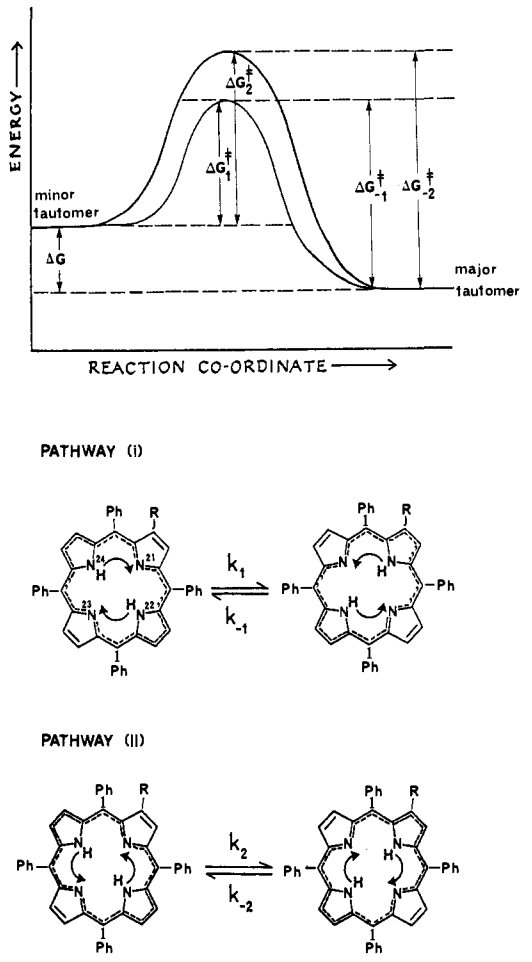

Figure 7. Energy profile for proton transfer in 2-substituted 5,10,15,20-tetraphenylporphyrins.

Table IV. Activation Parameters for Tautomerism in 2-Substituted 5,10,15,20-Tetraphenylporphyrins

compd no.	R	$\Delta G_1^{\ddagger}{}_{255}$,[a] kJ·mol^{-1}	$\Delta G_2^{\ddagger}{}_{255}$,[b] kJ·mol^{-1}	ΔG,[e] kJ·mol^{-1}
17	CH_3	47.4 ± 0.7	54.5 ± 0.9	−2.5
15	NH_2	45.6 ± 0.6	55.5 ± 0.8	−1.3
14	$CH{=}CH_2$	45.7 ± 0.6	*d*	−1.0
13	CH_2OH	45.8 ± 0.6	*d*	−0.8
1	H	50.7[c]	50.7[c]	0
11	$NHCOCH_3$	47.2 ± 0.7	*d*	1.4
9	OCH_3	47.8 ± 0.7	*d*	2.3
10	SPh	47.1 ± 0.7	*d*	2.0

[a] Extrapolated from $\Delta G^{\ddagger}_{225}$ in Table I. [b] Extrapolated from $\Delta G^{\ddagger}_{280}$ in Table II. [c] See text. [d] Data not obtainable by DNMR (see text). [e] Ground-state energy difference between tautomers $\Delta G = RT \ln [P2a/P2b]$; *P2a* and *P2b* at 255 K from line shape results.

activation energies $\Delta G_1^{\ddagger}$ and $\Delta G_2^{\ddagger}$, the data were extrapolated to 255 K (Table IV). Kinetic data for 5,10,15,20-tetraphenylporphyrin **1** at 255 K are also included in Table IV.[25]

Exchange Processes. The tautomerism **2a** ⇄ **2b** in a 2-substituted 5,10,15,20-tetraphenylporphyrin, **2**, involves a net two-proton transfer which can be viewed essentially as occurring via two pathways: (i) N-24 ⇄ N-21 and N-22 ⇄ N-23 or (ii) N-24 ⇄ N-23 and N-22 ⇄ N-21. The two nonequivalent pathways result from the asymmetry in the porphyrin associated with the R substituent. The results in Tables II and III indicate that there is a remarkable directional preference for the proton transfer in 2-substituted 5,10,15,20-tetraphenylporphyrins. *In all of the porphyrins studied in this work, proton transfer via pathway i is much more facile than via pathway ii.*

The energy barrier, $\Delta G_1^{\ddagger}$ (proton transfer from N-24 to N-21 and proton transfer from N-22 to N-23), in porphyrins **15** and **17** is less than the energy barrier $\Delta G_2^{\ddagger}$ (proton transfers N-24 to N-23 and N-22 to N-21) (Figure 7). While measurement of both energy barriers was not possible in porphyrins **9**, **10**, **11**, **13**, and **14**, it is reasonable to assume that proton transfer in these porphyrins can be represented by a similar energy profile, differing only in the relative ground-state energies of the tautomers. Relative to the unsubstituted parent, 5,10,15,20-tetraphenylporphyrin **1**, 2-substitution lowers the energy of activation for proton transfer by pathway i and increases the energy of activation for proton transfer by pathway ii (Table IV, Figure 7).

Rationalization of the results involves consideration of the effect of the substituent in the 2-position on the framework within which the protons move. The origin of the directionality in the proton transfer could be steric and/or electronic in nature.

Substituents on the aryl rings, as well as in the β-pyrrolic positions, have been shown to transmit electronic effects to the inner nitrogens. The tautomerism involves N–H bond breakage/formation and would be expected to be somewhat dependent on the relative acidities of the nitrogens. Indeed, it has been noted that the introduction of certain β-substituents causes significant changes (up to ca. 3 pK_a units) to the basicities of the inner nitrogens.[26] While the effect of one β-pyrrolic substituent would be expected to be transmitted primarily to the nitrogen in the same ring, the other nitrogens and any transition state for proton migration would also be influenced to some degree. The activation parameters were obtained in porphyrins in which the electronic nature of the substituent was varied considerably. However, any electronic contribution of the substituent to the energy barriers $\Delta G_1^{\ddagger}$ and $\Delta G_2^{\ddagger}$ is not apparent. While the higher energy barrier, $\Delta G_2^{\ddagger}$ was obtained in only two cases, certainly the lower energy barrier, $\Delta G_1^{\ddagger}$, shows no obvious relation to the electronic nature of the 2-substituent. This was also the case in the thermodynamics of the tautomeric equilibrium, **2a** ⇄ **2b**, where it was proposed that a steric component probably contributes to the stabilization of a given tautomer since the results did not parallel any substituent scale.[15]

A steric effect might be important; calculations by Sarai[12] on 5,10,15,20-tetraphenylporphyrin **1** have shown that the deformation energy of the porphyrin skeleton due to tautomerism is large, and hence tautomerism is always accompanied by relatively large distortions of molecular structure. In particular, appreciable differences are found in the bond angles and lengths in the pyrrole ring with the central proton attached compared to the unprotonated ring during proton transfer. The upfield chemical shifts of the ortho protons in the NMR spectra of **3**–**18**[15] indicate the presence of a steric effect between the substituent and the *peri*-phenyl ring. In view of the fact that tautomerism is accompanied by heavy atom (skeletal carbons and nitrogens) movement,[12] a β-pyrrolic substituent would be expected to have a steric influence on the exchange process. There are several possible ways this could occur.

The interaction of a β-substituent with the adjacent meso position may restrict the flexibility of the framework in this portion of the molecule relative to the rest of the molecule. Examination of CPK molecular models shows that such an interaction would distort the geometry of the porphyrin, shortening the N-24 to N-21 bond distance by opening the angle between the substituent and the *peri*-phenyl ring. Alternatively, steric hindrance between the substituent and the *peri*-phenyl ring may twist this ring into a more

(25) The value of k for **1** was obtained from an Eyring analysis of the rate constants summarized in ref 10a (excluding $T_{1\rho}$ measurements)[11b] which were obtained by line shape analysis in the temperature range 190–320 K. However, in 5,10,15,20-tetraphenylporphyrin, the rate processes designated k_1 and k_2 in this study are identical. Hence if one labels the interior nitrogens in **1**, the measured rate constant k for proton tautomerism represents the sum of k_1 and k_2. It should be noted that all previous studies on symmetrical porphyrins do not appear to take into account the fact that the exchange takes place via two degenerate pathways. Hence the reported activation parameters do not correspond to a physical process. The value of k for **1**, at 255 K (527 s^{-1}), was divided by 2 to give estimates of $\Delta G_1^{\ddagger} = \Delta G_2^{\ddagger}$.

(26) Smith, K. M. In *Porphyrins and Metalloporphyrins*; Smith, K. M., Ed.; Elsevier: Amsterdam, 1975; pp 11–13.

orthogonal orientation than the other three phenyl rings in the molecule. Such a change would reduce conjugation of this ring with the porphyrin aromatic π-system and distort the geometry of the molecule. The extent of such interactions remains speculation since there is no X-ray data or calculations as to the structure of 2-substituted 5,10,15,20-tetraphenylporphyrins.

Mechanism of Proton Transfer. The results of previous studies on tautomerism in symmetrical tetraarylporphyrins are consistent with simultaneous migration of the two protons involving a symmetrical transition state.[6] Large temperature-dependent deuterium isotope effects (48 ± 14 at 243 K) have been observed in a range of para-substituted tetraarylporphyrins.[6] The tautomerism is solvent, concentration, and aryl ring substituent independent[6] and above 200 K does not involve proton tunneling.[12]

Our data show that asymmetric porphyrins exhibit the same kinetic properties as the symmetrical porphyrins. Although our data show net two-proton transfer between the tautomers, the possibility of asynchronous movement on a molecular level cannot be excluded. An estimate of the kinetic isotope effect on k_1 (i.e., proton transfer from N-24 to N-21 and from N-22 to N-23) was obtained for 2-methoxy-5,10,15,20-tetraphenylporphyrin **9**. Line shape analysis of the N–H and methoxyl resonances of **9** was performed in the temperature range 200–235 K, while analysis of the methoxyl region of the deuteriated derivative produced values of k_1 in the range 245–285 K. An isotope effect of $k_H/k_D = 30 \pm 3$ at 242 K was obtained. This is comparable to the values reported for symmetrical tetraarylporphyrins[5c,6] and suggests that the transition-state structures for tautomerism in **1** and **2** are similar. Comparison of the activation parameters also strongly suggests that a similar mechanism operates in both systems.

Arrhenius plots of the kinetic data were linear over the range 200–300 K and show no evidence for proton tunneling. Hennig and Limbach[10] have proposed the existence of a temperature-independent (5.0 ± 0.5 s^{-1}) proton tunneling in 5,10,15,20-tetraphenylporphyrin **1**. Mosely and Stilbs[11] have argued against this proposal. The fact that in our work, exchange rates in 2-substituted porphyrins of less than 5 s^{-1} were measured (Tables I and II) by both DNMR and saturation transfer experiments implies that any temperature-independent tunneling is insignificant (on the NMR time scale) above 190 K. Proton tunneling in asymmetric systems involving an asymmetric double well potential is inherently less likely than in symmetrical systems, as only that part of the barrier which lies above both the initial and final states is available for tunneling.[27] This fact, taken together with the similarity of kinetic data in unsubstituted and 2-substituted tetraphenylporphyrins, further suggests that tunneling is absent in both systems.

Conclusions

(i) The tautomeric exchange, **2a** ⇄ **2b**, in 2-substituted 5,10,15,20-tetraphenylporphyrins involves two distinct exchange processes which are detectable by saturation transfer experiments and DNMR spectroscopy.

(ii) In all porphyrins studied, proton transfer involves a net two-proton transfer between tautomers in which the two hydrogens reside on diagonally opposite nitrogens.

(iii) Irrespective of the nature of the substituent, there is a directional preference for proton transfer N-24 ⇄ N-21 and N-22 ⇄ N-23; the alternative exchange N-24 ⇄ N-23 and N-21 ⇄ N-22 is much slower.

(iv) The cause of the observed directionality of the proton transfer has not been unequivocally established. The energy barriers show no obvious correlation to the electronic or steric nature of the substituent.

(v) The activation parameters for tautomerism in 2-substituted porphyrins **9–18** and an isotope effect in porphyrin **9** are essentially the same as those observed in symmetrical porphyrins. This suggests that the mechanism of proton transfer is similar in both symmetrical and asymmetrical systems.

(vi) No evidence for proton tunneling above 190 K was found.

(vii) The results obtained in this study show further that asymmetric porphyrins inherently provide more information on tautomerism than is available from the study of symmetrical porphyrins.

Acknowledgment. We thank the Australian Research Grants Scheme for financial support (to M.J.C.) and the Australian Government for a Commonwealth Postgraduate Award (to M. M.H.).

Registry No. 9, 95519-30-5; **10**, 82945-69-5; **11**, 82945-62-8; **12**, 102305-84-0; **13**, 81914-52-5; **14**, 42259-23-4; **15**, 82945-59-3; **16**, 102305-85-1; **17**, 102305-86-2; **18**, 102305-87-3.

Supplementary Material Available: Data used to obtain values in Tables II and III (17 pages). Ordering information is given on any current masthead page.

(27) Bell, R. P. *Chem. Soc. Rev.* **1974**, *3*, 513.

Kinetics of the Thermal Reduction of Methylviologen in Alkaline Aqueous and Methanolic Solutions

Vivian Novakovic and Morton Z. Hoffman*

Contribution from the Department of Chemistry, Boston University, Boston, Massachusetts 02215. *Received October 24, 1986*

Abstract: Methylviologen (MV^{2+}) is reduced to $MV^{\bullet+}$ in alkaline aqueous and methanolic solutions in the absence of air. In aqueous solution, the initial rate of $MV^{\bullet+}$ formation (R_i) obeys the following rate law: $R_i = k_{obsd}[MV^{2+}]^2[OH^-]^2$; $k_{obsd} = 0.12$ M^{-3} min^{-1} at 25.0 °C with $E_a = 58$ kJ mol^{-1}. A mechanism is proposed whereby the initial phase of the reaction occurs via the successive attack of OH^- on the 2- and 2′-positions of the aromatic rings, followed by the reduction of MV^{2+} by the electron-rich double pseudobase. In methanolic solution, the rate law is $R_i = k_{obsd}[MV^{2+}]^{1/2}[CH_3O^-]^2$; $k_{obsd} = 4.9 \times 10^2$ $M^{-3/2}$ min^{-1} at 25.0 °C with $E_a = 95$ kJ mol^{-1}. It is suggested that MV^{2+} exists in methanolic solutions at the concentrations employed mainly as a dimeric aggregate, $(MV^{2+})_2$. the proposed mechanism involves an equilibrium between MV^{2+} and $(MV^{2+})_2$, with only MV^{2+} being reactive toward the formation of the pseudobase with CH_3O^-. Exposure of $MV^{\bullet+}$ to O_2 results in the formation of luminescent (λ_{em} 525 nm) and absorbing (λ_{max} ~380 nm) species via secondary reactions involving H_2O_2, which is formed slowly from the disproportionation of $O_2^{\bullet-}$.

Methylviologen (1,1′-dimethyl-4,4′-bipyridinium dication; MV^{2+}) is the archetypical electron relay in systems that serve as models for the photochemical storage and conversion of solar energy;[1] in addition, MV^{2+} is an important herbicide[2] and bio-

0002-7863/87/1509-2341$01.50/0